International Forum on Aeroelasticity and Structural Dynamics
IFASD 2019
9-13 June 2019, Savannah, Georgia, USA

DISCRETE TIME STATE-SPACE AEROSERVOELASTIC MODELING USING FUN3D

Z. Wang [1], D. Sarhaddi [1], and P.C. Chen [1]

[1] ZONA Technology, Inc.
Scottsdale, AZ, 85258 USA
zhicun@zonatech.com
darius@zonatech.com
pc@zonatech.com

Keywords: state space, aeroelasticity, aeroservoelastic, system identification, CFD, subspace realization

Abstract: In this paper, a discrete time state-space aeroservoelastic modeling technique using FUN3D is discussed. A subspace realization algorithm is utilized to identify the individual aerodynamic systems, i.e., due to the structural deformations (modal coordinates), control surface deflections and/or discrete gust, respectively. This subspace realization algorithm has been implemented in our flight test data processing application called ZAMS+ within IADS environment and proved to be an efficient and robust system identification tool in real time. The dataset needed for the aerodynamic system identifications are obtained by a wrapper program, called OVERFUN, driving the underlying FUN3D solver. The routines of the subspace realization algorithm are incorporated within the OVERFUN program to identify the individual aerodynamic sub-systems, and thereafter they are coupled with the structural equation of motion represented in modal space and the actuator model to yield the conventional state-space forms of aeroelastic model and plant model. The Benchmark Active Control Technology (BACT) wing is studied as the example case to demonstrate the presented methodology. The obtained state-space models are used to compute the frequency response of an accelerometer with respect to the trailing edge flap and the upper spoiler, and the results are compared to the test data and solutions by others.

1 INTRODUCTION

Maneuver and gust loads on aircraft usually are two of the critical design loads that dominate the structural design. To avoid the weight penalty for reducing the dynamic loads, e.g., both Boeing 787 and Airbus A320 are equipped with a maneuver and gust load alleviation control law using the aileron and spoiler to provide the control authority. The design of an efficient maneuver and gust load alleviation controller requires an enormous amount of wind tunnel testing and flight testing to tune the control laws. An accurate aeroservoelastic (ASE) model would greatly enhance the early design of the controller and reduce wind tunnel and flight test time. The examples of the afore mentioned Boeing 787 and Airbus A320 demonstrate the importance of the availability of a plant model in the early design stages, which allows the designer to rapidly design a control system and to evaluate its performance for flutter suppression and gust load alleviation (GLA).

The current ASE methodology used by the industry typically starts from the generation of the generalized aerodynamic forces (GAF). These GAFs are first computed in the frequency domain ($i\omega$), for example by ZAERO [1] employing the linear potential unsteady

aerodynamic methods or the Doublet Lattice Method [2], or by the unstructured CFD-based ZULUS code [3]. By applying the Rational Function Approximation (RFA) technique (i.e., Roger's [4] or Minimum-State method [5]), these GAFs are converted to the Laplace domain in the form of rational functions. Thereafter, the aeroelastic equation of motion can be easily cast into state-space form. Apparently, the key component of this approach is the computation of the GAFs in the frequency domain. ZULUS employs the background solution obtained by NASA high-fidelity Navier-Stokes (N-S) flow solver, FUN3D [6], and then the linearized Euler solver is implemented to compute GAFs. The convenience of the transpiration boundary condition enables the consideration of control surfaces without resorting to moving the mesh. However, the viscous effect is neglected by the linearized Euler solver.

On the other hand, CFD-based reduced order modeling (ROM) has been an active research area. Among them, the linearized reduced-order modeling approaches rely on linearization of the nonlinear unsteady aerodynamic flow equations, assuming that the amplitude of the unsteady motion is limited to small perturbations about the nonlinear steady-state flow condition. Various approaches of linearized ROMs, such as Auto-Regressive-Moving-Average (ARMA) [7], first order Volterra Kernel [8], Impulse Response method [9], etc., can be broadly found in literature. However, few of them are geared towards the controller design oriented plant modeling, i.e., to obtain a plant model with control surface actuator modeling and gust excitations.

In this paper, a discrete time state-space aeroservoelastic modeling technique using FUN3D is discussed. The subspace realization algorithm [10, 11] will be utilized to identify the individual aerodynamic systems, i.e., due to the structural deformations (modal coordinates), control surface deflections and/or discrete gust, respectively. The dataset needed for the aerodynamic system identifications are obtained by a wrapper program, called OVERFUN [12, 13], driving the underlying FUN3D solver. Once all three sub aerodynamic system are identified, they are coupled with the structural equation of motion represented in modal space and actuator models to yield the conventional state-space forms of aeroelastic model and plant model (see Figure 1 for the block diagram illustration), as described in the following.

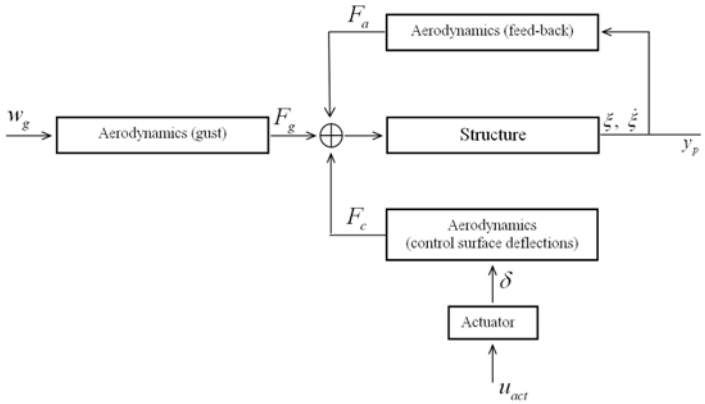

Figure 1: Block diagram of ASE plant model.

2 FORMULATION OF DISCRETE TIME STATE-SPACE AEROELASTIC MODEL

The structural equation of motion in modal space is represented as:

$$M_{hh}\ddot{\xi} + C_{hh}\dot{\xi} + K_{hh}\xi = q_\infty \left\{ F_a\left(\xi\right) + F_c\left(\delta\right) + F_g\left(w_g\right) \right\} \tag{1}$$

where M_{hh}, C_{hh}, and K_{hh} are the generalized structural mass, damping and stiffness matrices, respectively. ξ is the structural modal or generalized coordinate. F_a, F_c, and F_g are the generalized aerodynamic force (GAF) vectors due to structural deformations, control surface deflections and gust, respectively.

Equation (1) can be casted into first order ordinary differential equation (ODE) as the following:

$$\frac{d}{dt}x_s = \bar{A}_s x_s + q_\infty \bar{B}_s \left(F_a + F_c + F_g\right) \tag{2}$$

where $x_s = \left[\xi \quad \dot{\xi}\right]^T$ represents the structural states; and

$$\bar{A}_s = \begin{bmatrix} 0 & I \\ -M_{hh}^{-1}K_{hh} & -M_{hh}^{-1}C_{hh} \end{bmatrix}; \quad \bar{B}_s = \begin{bmatrix} 0 \\ M_{hh}^{-1} \end{bmatrix} \tag{3}$$

Converting Equation (2) from continuous time domain to discrete time domain and adding the sensor information (e.g., displacements, velocities or accelerations at structural grids), we arrive at the discrete time state space form:

$$\begin{aligned} x_s(k+1) &= A_s x_s(k) + q_\infty B_s\left(F_a + F_c + F_g\right) \\ y_s(k) &= C_s x_s(k) + q_\infty D_s\left(F_a + F_c + F_g\right) \end{aligned} \tag{4}$$

where *k* denotes the discrete time step index. The discrete time system matrices, A_s, and B_s with a given time step size Δt, are obtained from:

$$A_s = \exp\left(\bar{A}_s \Delta t\right); \; B_s = \int_0^{\Delta t} \bar{B}_s \exp\left(\bar{A}_s \tau\right) d\tau \tag{5}$$

Next, the discrete time state-space models for F_a, F_c, and F_g are sought after one by one. Relying on the subspace realization algorithm, a discrete time state-space model can be obtained for the aerodynamic forces due to structural deformations. The state-space equations for $F_a(\xi)$ are as follows:

$$\begin{aligned} x_a(k+1) &= A_a x_a(k) + B_a \xi(k) \\ F_a(k) &= C_a x_a(k) + D_a \xi(k) \end{aligned} \tag{6}$$

where x_a is the aerodynamic states; A_a, B_a, C_a, and D_a are the identified time invariant system matrices.

Similarly, we can obtain the state space models for aerodynamic forces due to control surface deflections, $F_c(\delta)$:

$$\begin{aligned} x_c(k+1) &= A_c x_c(k) + B_c \delta(k) \\ F_c(k) &= C_c x_c(k) + D_c \delta(k) \end{aligned} \tag{7}$$

where x_c is the control surface aerodynamic states; A_c, B_c, C_c, and D_c are the identified system matrices for the aerodynamics due to control surface deflections.

Combining Equations (4), (6), and (7), and neglecting the aerodynamic forces due to gust for the time being, we have:

$$\begin{Bmatrix} x_s \\ x_a \\ x_c \end{Bmatrix}(k+1) = \begin{bmatrix} A_s + q_\infty B_s D_{aa} & q_\infty B_s C_a & q_\infty B_s C_c \\ B_a & A_a & 0 \\ 0 & 0 & A_c \end{bmatrix} \begin{Bmatrix} x_s \\ x_a \\ x_c \end{Bmatrix}(k) + \begin{bmatrix} q_\infty B_s D_c \\ 0 \\ B_c \end{bmatrix} \delta(k) \tag{8}$$

By denoting:

$$x_{ae} = \begin{Bmatrix} x_s \\ x_a \\ x_c \end{Bmatrix}; \quad u_{ae} = \delta \tag{9}$$

$$A_{ae} = \begin{bmatrix} A_s + q_\infty B_s D_{aa} & q_\infty B_s C_a & q_\infty B_s C_c \\ B_a & A_a & 0 \\ 0 & 0 & A_c \end{bmatrix}; \qquad B_{ae} = \begin{bmatrix} q_\infty B_s D_c \\ 0 \\ B_c \end{bmatrix} \tag{10}$$

we obtain the conventional form of discrete time open-loop aeroelastic equation of motion (AEMODEL):

$$x_{ae}(k+1) = A_{ae} x_{ae}(k) + B_{ae} u_{ae}(k) \tag{11}$$

3 FORMULATION OF DISCRETE TIME PLANT MODEL

We now consider the actuator models. The dynamic model of an actuator driving a control surface is normally specified by a transfer function having the form:

$$\delta = \frac{a_0}{s^3 + a_2 s^2 + a_1 s + a_0} u_{act} \tag{12}$$

where u_{act} is the servo-commanded (actuator input) control surface deflection.

A higher order actuator dynamics can be defined by adding cascade transfer function as a part of the control system. A state-space realization of Equation (12) is:

$$\{\dot{x}_{act}\} = \begin{bmatrix} 0 & 1 & 0 \\ 0 & 0 & 1 \\ -a_0 & -a_1 & -a_2 \end{bmatrix} \{x_{act}\} + \begin{Bmatrix} 0 \\ 0 \\ a_0 \end{Bmatrix} u_{act} \tag{13}$$

where $x_{act} = \begin{bmatrix} \delta & \dot{\delta} & \ddot{\delta} \end{bmatrix}^T$.

Equation (13) in turn can be converted in to discrete time form:

$$x_{act}(k+1) = A_{act}x_{act}(k) + B_{act}u_{act}(k) \tag{14}$$

For a system with more than one actuators, the state-space model with the same form of Equation (14) of all the actuators can be arranged so that total actuator state vector x_{act} equals to the input vector u_{ae} in Equation (11). Combining Equation (11) and (14) together leads to:

$$\begin{aligned} \begin{Bmatrix} x_{ae} \\ x_{act} \end{Bmatrix}(k+1) &= \begin{bmatrix} A_{ae} & B_{ae} \\ 0 & A_{act} \end{bmatrix} \begin{Bmatrix} x_{ae} \\ x_{act} \end{Bmatrix}(k) + \begin{bmatrix} 0 \\ B_{act} \end{bmatrix} u_{act}(k) \\ y_{ae}(k) &= \begin{bmatrix} C_{ae} & D_{ae} \end{bmatrix} \begin{Bmatrix} x_{ae} \\ x_{act} \end{Bmatrix}(k) \end{aligned} \tag{15}$$

By denoting:

$$\begin{aligned} & x_p = \begin{bmatrix} x_{ae} & x_{act} \end{bmatrix}^T; \qquad y_p = y_{ae}; \qquad u_p = u_{act} \\ & A_p = \begin{bmatrix} A_{ae} & B_{ae} \\ 0 & A_{act} \end{bmatrix} \\ & B_p = \begin{bmatrix} 0 \\ B_{act} \end{bmatrix} \\ & C_p = \begin{bmatrix} C_{ae} & D_{ae} \end{bmatrix} \end{aligned} \tag{16}$$

we obtain the plant model in discrete time state space form:

$$\begin{aligned} x_p(k+1) &= A_p x_p(k) + B_p u_p(k) \\ y_p(k) &= C_p x_p(k) \end{aligned} \tag{17}$$

The plant state-space equations are ready for control system design or to be connected with a given control system to perform the closed-loop ASE analysis.

4 OVERFUN PROGRAM

4.1 OVERFUN Overview

It is known that the steady aerodynamic solution has a large influence on the unsteady aerodynamic solution especially in the nonlinear flow conditions. Therefore, it is of importance that the unsteady aerodynamic computation starts from a statically equilibrium trim condition. A program named as OVERFUN is initially developed to perform both determined and over-determined trim analyses with static aeroelastic (STAERO) effects. OVERFUN drives the high-fidelity Navier-Stokes (N-S) solver in FUN3D execution to obtain the aerodynamic stability derivatives required by trim analyses. Based on an optimization formulation, the over-determined trim analysis can determine the optimum control surface scheduling of multiple control surfaces to achieve the best aerodynamic efficiency of the aircraft. At the critical loads flight conditions, the optimum control surface scheduling can minimize the design loads; leading to a lighter and more flexible structural design. At cruise conditions, the optimum control surface scheduling computed by the over-determined trim analysis can aeroelastically deform the more flexible structure to an optimum shape for induced drag minimization. OVERFUN's trim or static aeroelastic analysis solution provides an initial background solution accounting for static aeroelastic effects, around which a

linearized aerodynamic reduced order model can be derived.

OVERFUN uses bulk data card format as input the same way as ZONA's ZAERO program. It consists of various modules, e.g., INIT module for initialization of database, IFP module for processing input deck, FEM module for processing the structural modal data, etc.

The wetted surface extracted from the CFD grid is then treated as the aerodynamic model seen by the OVERFUN program. The spline model establishes the displacement/force transfer matrix between the structural Finite Element Method (FEM) model and OVERFUN aerodynamic model. In addition to ZAERO's existing four spline methods: Thin Plate Spline, Infinite Plate Spline, Beam Spline, and Rigid Body Attachment method, another spline technique, Wendland Radial-Basis-Function (RBF), is developed as well. The structural modal shapes represented in the wetted surface are automatically written out according to FUN3D format and the file names follow FUN3D convention, i.e., `[project]_body1_mode[i].dat`, in order for FUN3D to perform aeroelastic analysis.

4.2 Consideration of Control Surface Kinematic Modes in OVERFUN/FUN3D

For OVERFUN/FUN3D to consider control surface deflection, the so-called kinematic modes must be defined.

The inputs to OVERFUN for the consideration of control surfaces include: (a) the CFD surface grids that belong to the control surface; (b) the hinge line location; and (c) control surface deflection command. The hinge line of a control surface is defined through the reference to a rectangular coordinate system's identification number, CID. The y-axis or z-axis of the rectangular coordinate system should pass through the hinge line of the control surface.

The control surface kinematic mode Φ_δ is such that all the grids lying on the control surface are given a unit deflection angle with respect to the hinge line while other grids outside of the control surface have zero motions. The deformation of surface mesh, $\{x_\delta(t)\}$, due to a given control surface deflection command, $\{\delta(t)\}$, can then be computed by the following Equation:

$$\{x_\delta(t)\} = [\Phi_\delta]\{\delta(t)\} \tag{18}$$

Equation (18) allows the deformed surface mesh remain continuous and coherent so that there is no discontinuous displacement occurring thus the "blended mesh" concept [14]. For FUN3D to conduct dynamic aeroelastic analysis, the structural modes projection into the wetted surface mesh are read in from files, `[project]_body1_mode[i].dat`. The first *NM* files of `[project]_body1_mode[i].dat` correspond to the *NM* number of structural modes, the next *NC* files correspond to the NC number of selected control surface kinematic modes. In this way, FUN3D would also see the control surface kinematic modes as the structural modes. At the same time, in the automatically generated `moving_body.input` file, the total number of nominal structural modes becomes *NM+NC*, and the artificial generalized mass and frequencies for the control modes are assigned as 1.0. The *moddfl* parameter for the control modes is always assigned as 5; it means that their "modal coordinates and velocity components" need be read from the "`rom_inputs_body1.dat`" file. The "`rom_inputs_body1.dat`' file is automatically generated by OVERFUN with the user specified excitations for the modal coordinates and the

control surfaces.

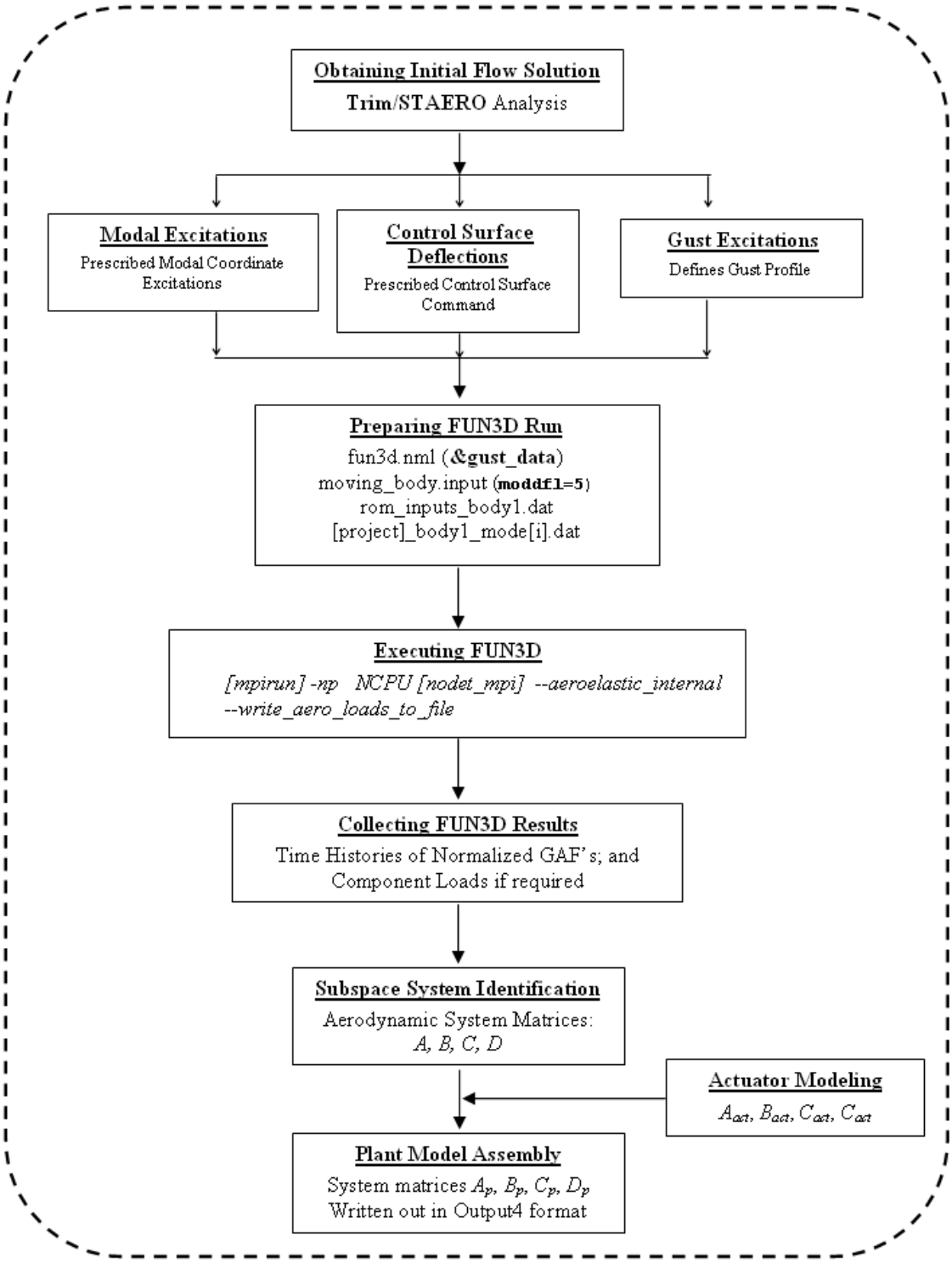

Figure 2: Program flow of discrete time state space plant model generation of OVERFUN SSMOD.

4.3 OVERFUN SSMOD Module

The discrete time state space aeroelastic and plant models are generated by a new module of OVERFUN, called SSMOD module. Because the NASA developed high fidelity Navier-Stokes flower solver FUN3D is utilized by OVERFUN, all the advantages/benefits possessed by FUN3D is retained, for example, the viscous effects can be well captured if desired.

The program flow of SSMOD is shown in Figure 2. OVERFUN SSMOD prepares all the necessary inputs and then drives the execution of FUN3D, subsequently conducts system identifications on the dataset obtained from the FUN3D results of generalized aerodynamic forces and sectional/component loads. Using subspace realization algorithm, the individual aerodynamic sub-systems, due to structural deformations (modal coordinates), control surface deflections, and/or gust velocities will be identified individually. Finally, the plant model is assembled by coupling the aerodynamic systems with the structural equations of motion represented in modal space along with the actuator models.

4.4 Excitation Signal

As mentioned, the dataset in terms of time histories of inputs and outputs needed for system identification process will be obtained by the program OVERFUN driving the execution of FUN3D flow solver. An important question is related to the excitation signal for each aerodynamic system's inputs: modal coordinates, or control surface deflections, or gust velocities.

From the point of view of system identification, the broader of the frequency contents the data include, the better the identified system represents the real system. As for this present study, we decide to use the low-pass-filtered white noise signals. The idea is to get a *NM* (i.e., the number of modes) number of uncorrelated series of white noise or random signals first, then each one of them is filtered through a low-pass filter to get rid of unnecessary higher frequency components. Such a filtered white noise signal is demonstrated in Figure 3. As seen in Figure 3(b), the higher frequency included in a white noise signal is cut off from the filtered signal.

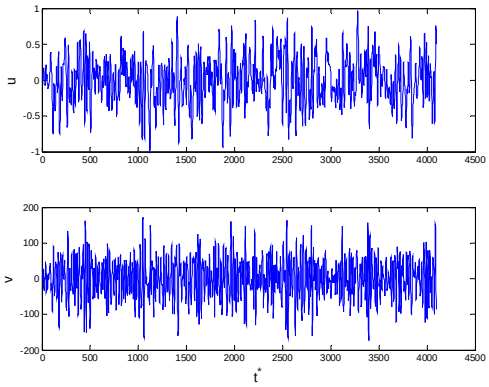

(a) Filtered random signal (u) and its velocity component (v)

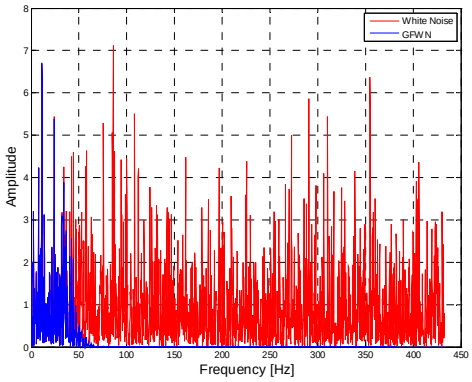

(b) Comparison of spectrum of the white noise signal and filtered signal

Figure 3: Demonstration of Gaussian filtered white noise excitation signal.

5 NUMERICAL RESULTS FOR THE BACT WING

5.1 The BACT Wing

To demonstrate the discrete time state-space modeling capability of OVERFUN SSMOD, we use the Benchmark Active Controls Technology (BACT) wing [15] as the numerical example. The BACT wing shown in Figure 4 is a rectangular wing with an NACA0012 airfoil section that was mounted on the pitch and plunge apparatus (PAPA), and was tested in the NASA Langley Transonic Dynamic Tunnel (TDT). The BACT wing has a trailing edge control surface (TE), an upper surface spoiler (US) and a lower surface spoiler. In the present paper,

the frequency responses of an accelerometer with respect to the TE and the upper spoiler control surfaces will be investigated.

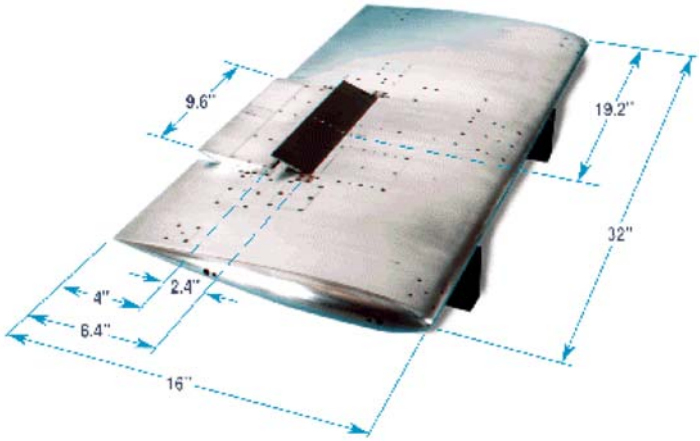

Figure 4: The BACT wing.

The structural model of the BACT wing only consists of two points, and two elastic modes (heaving and pitching) are considered. The generalized mass matrix M_{hh} includes the off diagonal terms and is given as follows:

$$M_{hh} = \begin{bmatrix} 0.4976 & -0.04976 \\ -0.04976 & 32.56 \end{bmatrix} \tag{19}$$

and the stiffness matrix K_{hh} is given as:

$$K_{hh} = \begin{bmatrix} 2.21583 \times 10^2 & 0 \\ 0 & 3.4764 \times 10^4 \end{bmatrix} \tag{20}$$

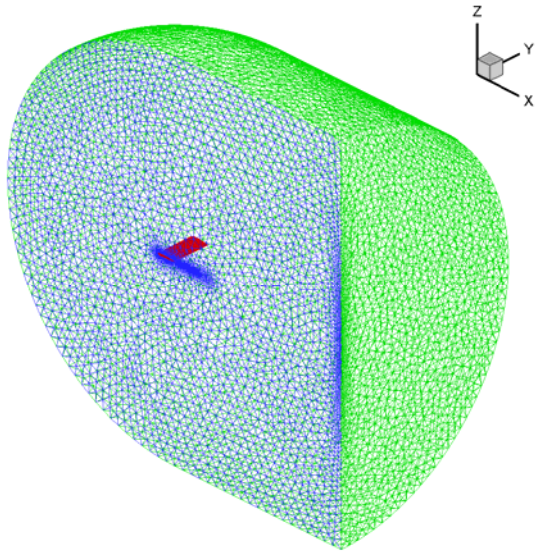

Figure 5: The unstructured grid for the BACT wing.

Figure 5 presents the unstructured grid for the BACT wing which consists of tetrahedrals. The rigid connection method via the ATTACH bulk data card is used to set up the spline matrix

between the structural model and the wing surface. The two mode shapes' projections on the wing surface of the CFD grid are shown in Figure 6.

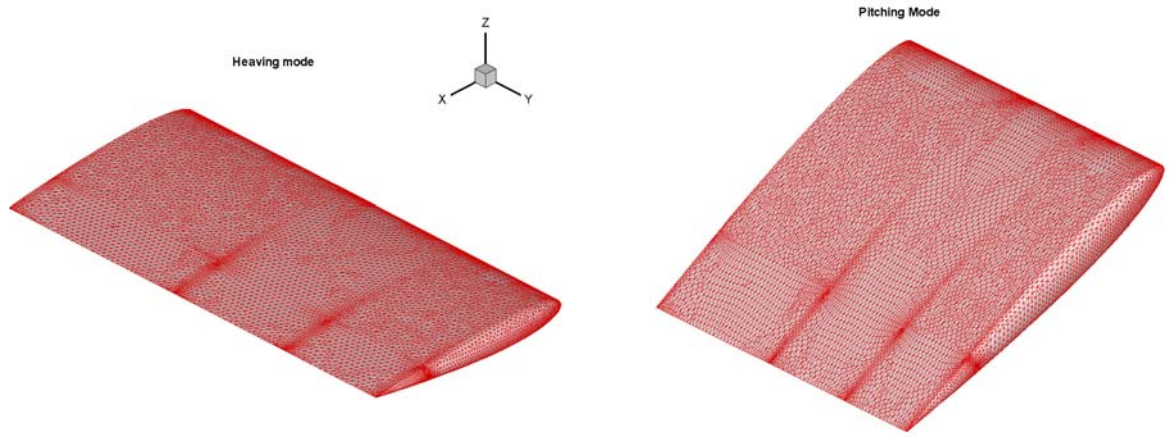

Figure 6: The two mode shapes of the BACT wing.

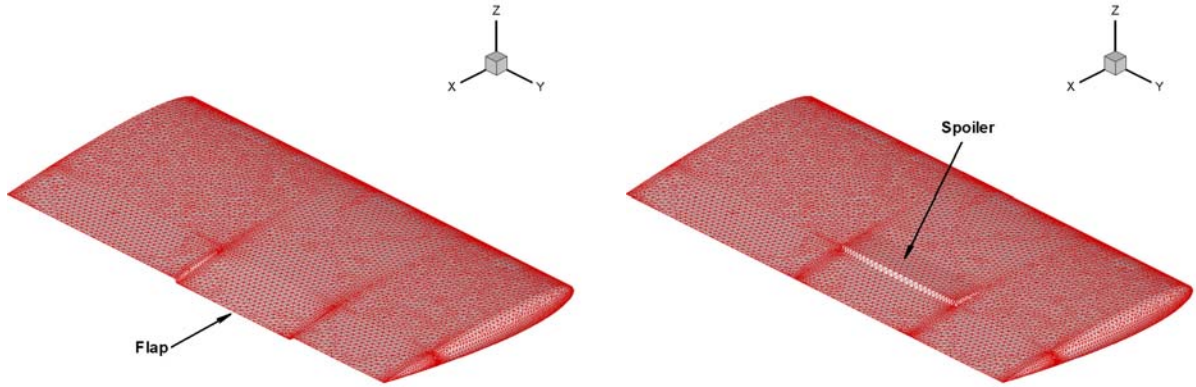

Figure 7: The TE Flap and the upper Spoiler control surfaces of the BACT wing.

The two control surfaces: the trailing edge flap and the upper spoiler are illustrated in Figure 7. The actuators attached to these two control surfaces have the same transfer function expressed by the following equation:

$$\frac{\delta}{u} = \frac{5.35\times10^7}{s^3 + 565.48s^2 + 2.13\times10^5 s + 5.35\times10^7} \tag{21}$$

5.2 Frequency Response due to the Trailing Edge Flap Input of the BACT Wing

The BACT wing during the TDT test includes an accelerometer located near the trailing edge of the BACT wing root (x = 13.196 inches). In this section, the accelerometer frequency response due to the trailing edge flap input is obtained by OVERFUN SSMOD, and compared with the TDT test data at Mach number of 0.61 and at dynamic pressure (q_∞) of 125 psf. The description of the TDT testing for the BACT wing is given in AIAA-96-3437-CP entitled "Modeling the Benchmark Active Control Technology Wind-Tunnel Model for Application to Flutter Suppression" by M. R. Waszak [16]. In Waszak's paper, he also computed the frequency domain responses of the BACT wing using the wind-tunnel measured aerodynamic stability derivatives.

Because the acceleration is not part of the structural states, the sensor output of the

acceleration must be derived from the structural equation of motion as follows:

$$\begin{aligned} y_s &= \phi_{hi}\ddot{\xi} \\ &= \phi_{hi}\left[-M_{hh}^{-1}C_{hh}\dot{\xi} - M_{hh}^{-1}K_{hh}\xi\right] + \phi_{hi}M_{hh}^{-1}q_\infty\left\{F_a(\xi) + F_c(\delta) + F_g(w_g)\right\} \\ &= \phi_{hi}\left[-M_{hh}^{-1}K_{hh} \quad -M_{hh}^{-1}C_{hh}\right]\begin{Bmatrix}\xi \\ \dot{\xi}\end{Bmatrix} + \phi_{hi}M_{hh}^{-1}q_\infty\left\{F_a(\xi) + F_c(\delta) + F_g(w_g)\right\} \end{aligned} \tag{22}$$

$$y_s = C_s x_s + q_\infty D_s\left\{F_a(\xi) + F_c(\delta) + F_g(w_g)\right\} \tag{23}$$

where ϕ_{hi} are the reduced mode shapes at the sensor locations, and

$$\begin{aligned} C_s &= \left[-\phi_{hi}M_{hh}^{-1}K_{hh} \quad -\phi_{hi}M_{hh}^{-1}C_{hh}\right] \\ D_s &= \left[\phi_{hi}M_{hh}^{-1}\right] \end{aligned} \tag{24}$$

Now, the acceleration sensor output in the state-space aeroelastic model can be computed by Equation (23).

The excitation signals of the two modal coordinates and the trailing edge flap deflection for OVERFUN SSMOD analysis along with the GAF solutions are shown in Figure 8 and Figure 9, respectively.

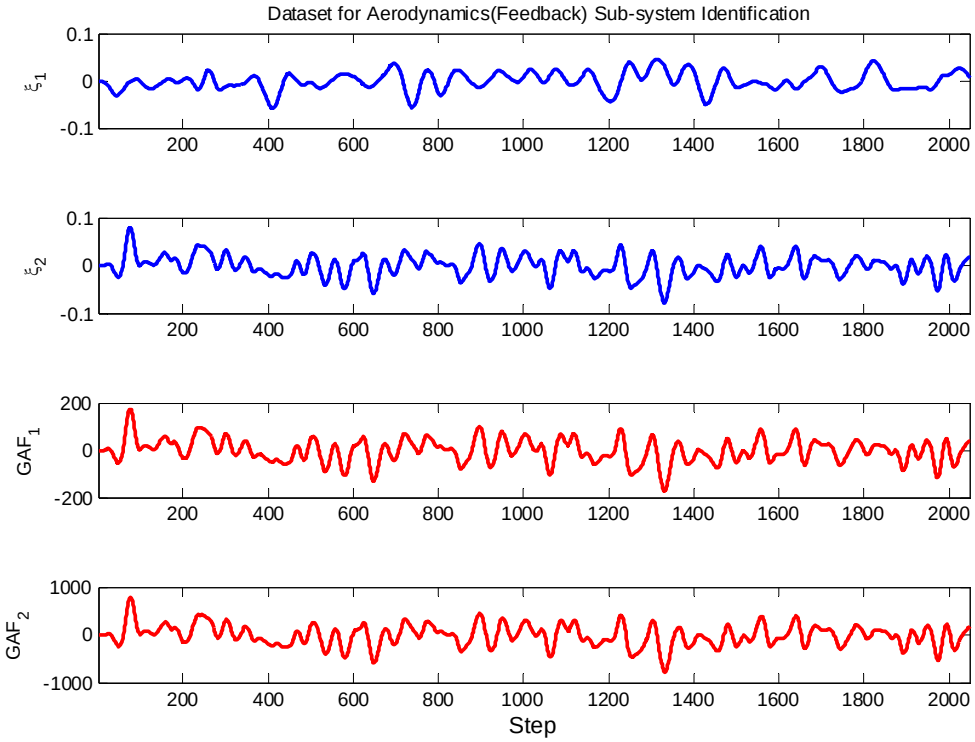

Figure 8: Data sets for the identification of the aerodynamic sub-system due to modal coordinates for the BACT wing (Mach=0.61, AoA=0).

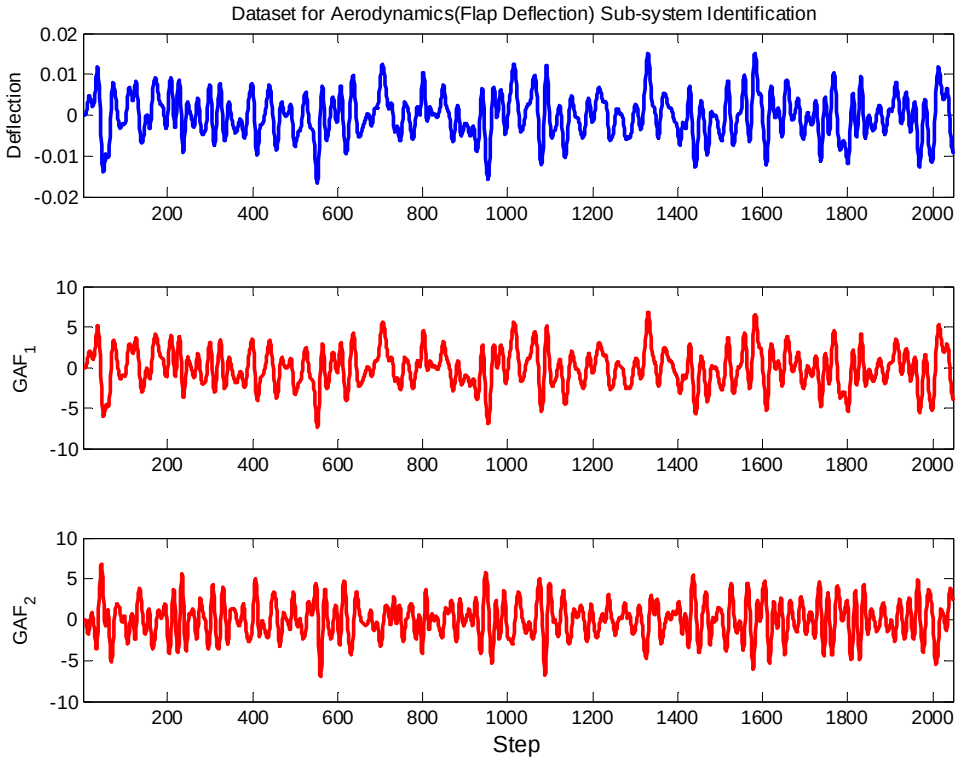

Figure 9: Data sets for the identification of the aerodynamic sub-system due to the Flap deflection for the BACT wing (Mach=0.61)

The SSMOD obtained AEMODEL without actuator models as represented by Equation (11) can be validated by comparing its modal coordinate solutions given any control surface deflection command with the direct FUN3D solutions. One such comparison is shown in Figure 10 for the BACT wing subject to a doublet control surface command. As we can see in the figure, an excellent agreement is achieved between the AEMODEL predictions and the direct solutions by FUN3D. Note that, the direct FUN3D solutions are obtained by using OVERFUN RETINAS module [13], which can drive FUN3D to perform dynamic aeroelastic analysis with control surface deflection inputs.

The sensor frequency response is obtained by a post-processing procedure in which a discrete time PLANT model are assembled first using the sub-system matrices output by OVERFUN SSMOD module, and then converted into continuous time domain, and finally the Matlab function `BODE` is used to yield the frequency response at the specified frequency range. The frequency response of the accelerometer due to trailing edge flap is plotted in Figure 11. The phase angle has been wrapped in between +/- 180 degrees. Also shown in Figure 11 are the frequency responses at the accelerometer due to the trailing edge flap input measured by TDT testing and computed by Waszak. Note that the natural frequencies of the BACT wing on the PAPA flexible mount system are 3.34 Hz for the plunge mode and 5.2 Hz for the pitch mode. However, the TDT test data shows that the frequency of the pitch mode is shifted from 5.2 Hz to approximately 4.5 Hz. Clearly, this frequency shift is due to the aeroelastic effects. Both Waszak's and OVERFUN SSMOD results capture this frequency shift except that the results obtained by Waszak over-predicts the magnitude of the peak at 4.5 Hz whereas the OVERFUN SSMOD predicted magnitude correlates better with the TDT data than the Waszak's result. This is probably because the Waszak's results are based on the wind-tunnel measured aerodynamic stability derivatives which are only valid at low frequency range. On

the other hand, the OVERFUN SSMOD generated unsteady aerodynamics cover a wider frequency range.

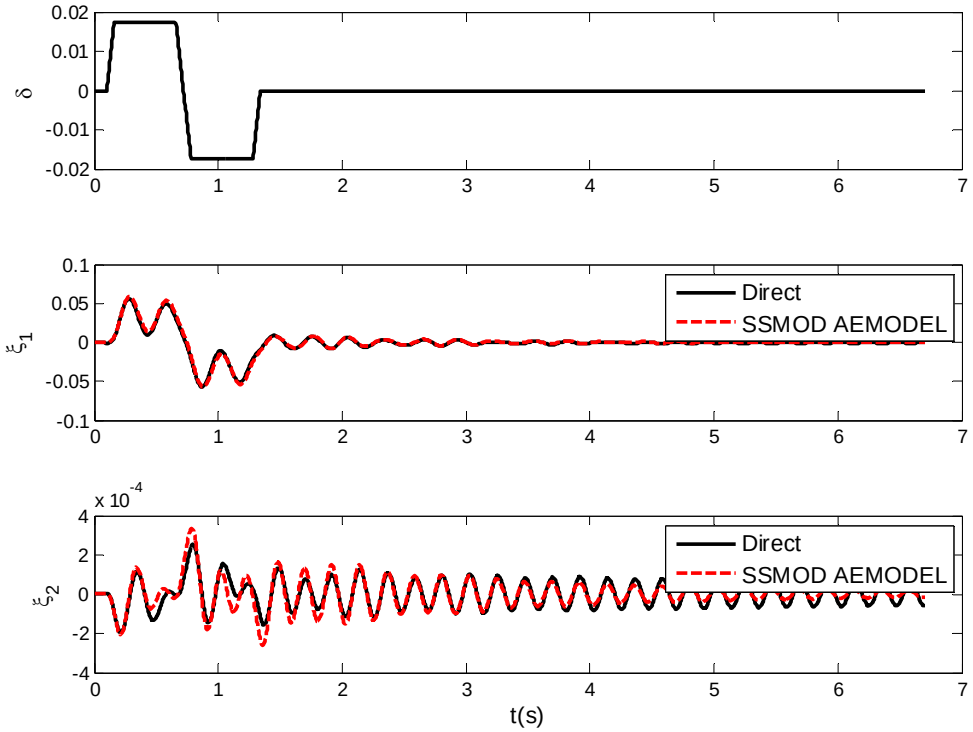

Figure 10: Modal coordinate solutions using the AEMODEL for the BACT wing subject to a doublet control command (Mach=0.61).

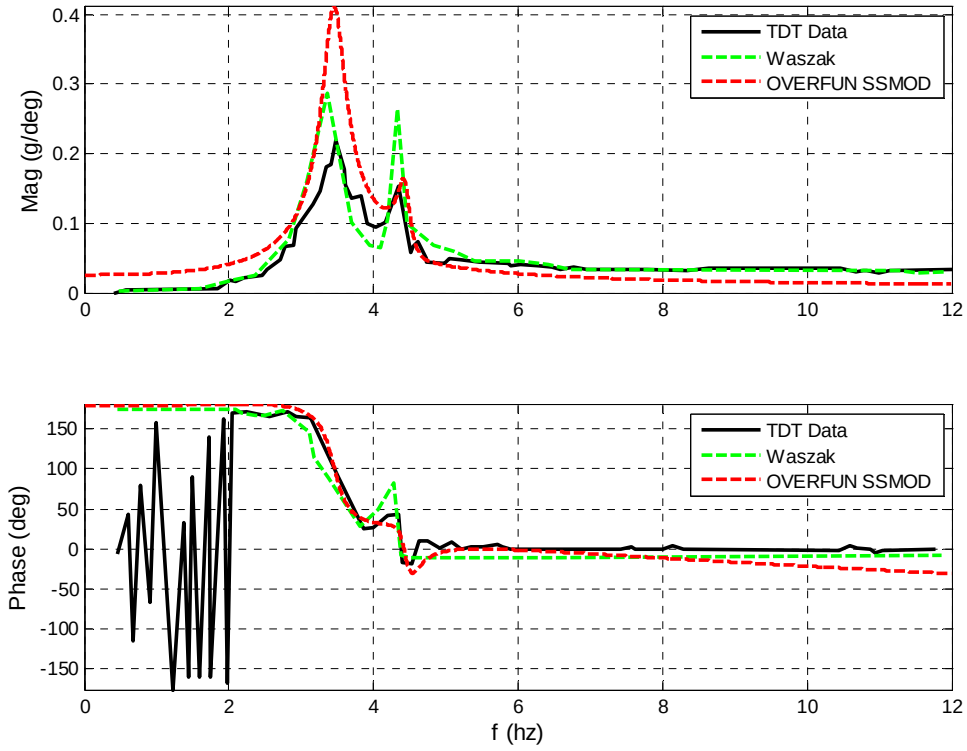

Figure 11: Frequency response of an accelerometer output to the trailing edge flap input of the BACT wing ($q_\infty = 125 psf$; Mach=0.61; AoA=0; mean Flap = 0).

5.3 Frequency Response due to the Upper Spoiler Input of the BACT Wing

Frequency response at the sensor of the BACT wing due to the upper spoiler input at a mean upper spoiler angle of 5 degrees, Mach number of 0.61 and the dynamic pressure of 125 psf was also measured by TDT testing and predicted by Waszak using the wind-tunnel measured aerodynamic stability derivatives. Because generating an unstructured mesh for such a complex geometry requires a tedious mesh generation effort, we again employ the blended mesh approach to model the BACT wing with a mean upper spoiler angle at 5° (see Figure 12(a)).

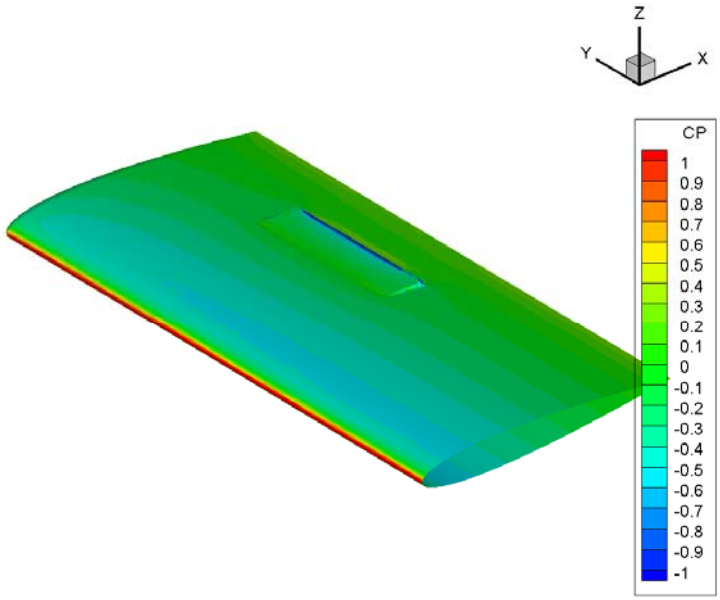

a) Cp Contour

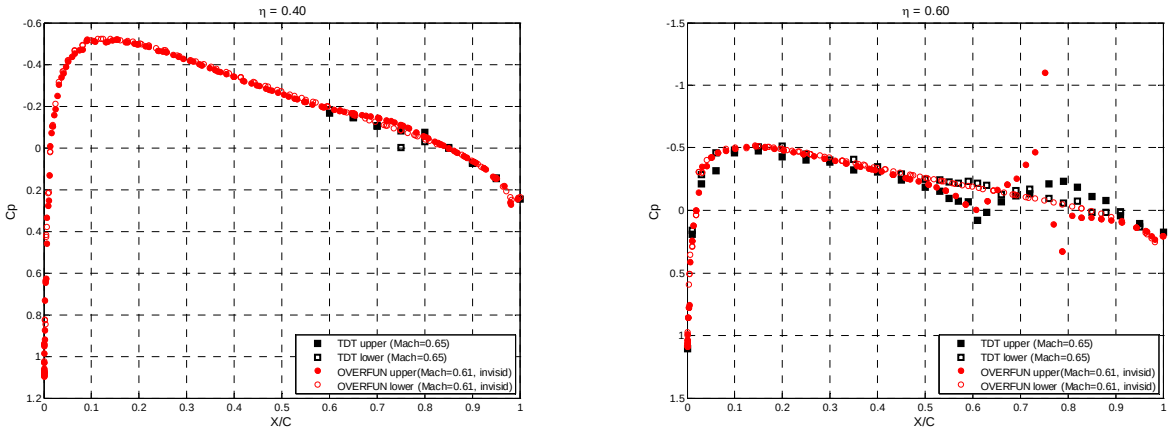

b) Cp vs. x

Figure 12: Mean steady solutions of the BACT wing (Mach =0.61; AoA=0; Spoiler = 5deg).

Using the blended mesh approach, the FUN3D predicted steady pressure distributions along span stations of 40% and 60 % are presented in Figure 12(b) along with the TDT measured data at a different but very close Mach number. Because the 40% span station is outside the

upper spoiler, the FUN3D predicted steady pressure distribution correlates well with the TDT measured data. However, at 60% span station which is along the center span of the upper spoiler, the FUN3D predicted pressure distribution largely departs from the TDT measured data especially on the spoiler and on the wing upper surface behind the spoiler. This is expected because in reality the regions below the spoiler and behind the spoiler on the wing are all immersed in separated flow. This flow physics cannot be truly captured by the blended mesh approach. However, it is still worthwhile to continuously investigate the applicability of OVERFUN SSMOD module for predicting the frequency response due to spoiler input using the blended mesh approach.

The procedure to generate the plant model for the spoiler input is same to that for the flap input. The excitation signals of the two modal coordinates and the upper spoiler deflection along with the GAF solutions are shown in Figure 13 and Figure 14, respectively.

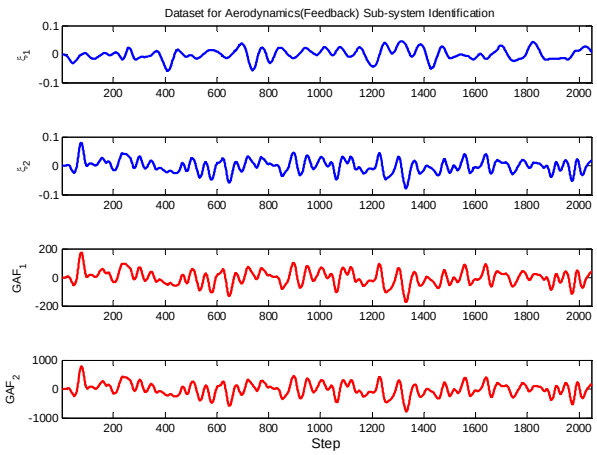

Figure 13: Data sets for the identification of the aerodynamic sub-system due to modal coordinates for the BACT wing (Mach =0.61; AoA=0; Spoiler = 5 deg).

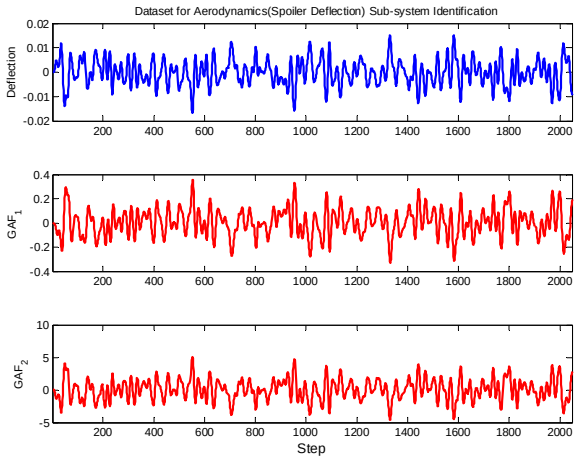

Figure 14: Data sets for the identification of the aerodynamic sub-system due to the Spoiler deflection for the BACT wing (Mach =0.61; AoA=0; Spoiler = 5 deg).

With the obtained state-space models obtained by OVERFUN SSMOD, the frequency response of the accelerometer due to upper spoiler input is presented in Figure 15 along with the TDT measurement and Waszak's prediction. Because of using the wind-tunnel measured aerodynamic stability derivatives, Waszak's result correlates well with the TDT measured data. On the other hand, the OVERFUN SSMOD result under-predicts the magnitudes at 3.3 Hz and 4.5 Hz. This is also expected because the blended mesh approach only models the upper surface of the spoiler and the lower surface of the spoiler is considered as a part of the interior of the wing. Therefore, the unsteady aerodynamic forces are generated only from the pressures on the upper surface of the spoiler; thereby under-predicting the unsteady aerodynamic forces provided by the upper spoiler.

While the frequency response due to flap input predicted by OVERFUN SSMOD presented in Figure 15 shows that the blended mesh approach for modeling the flap deflection can generate reasonably accurate plant model, the investigation of frequency response due to spoiler input suggests that the blended mesh approach for modeling the spoiler deflection cannot lead to a computational mesh, and the flow solver using this blended mesh cannot capture accurate flow physics. In future work, we will generate a computational mesh to model the physically deflected spoiler on the BACT wing and use OVERFUN SSMOD to re-investigate the frequency response due to the upper spoiler input.

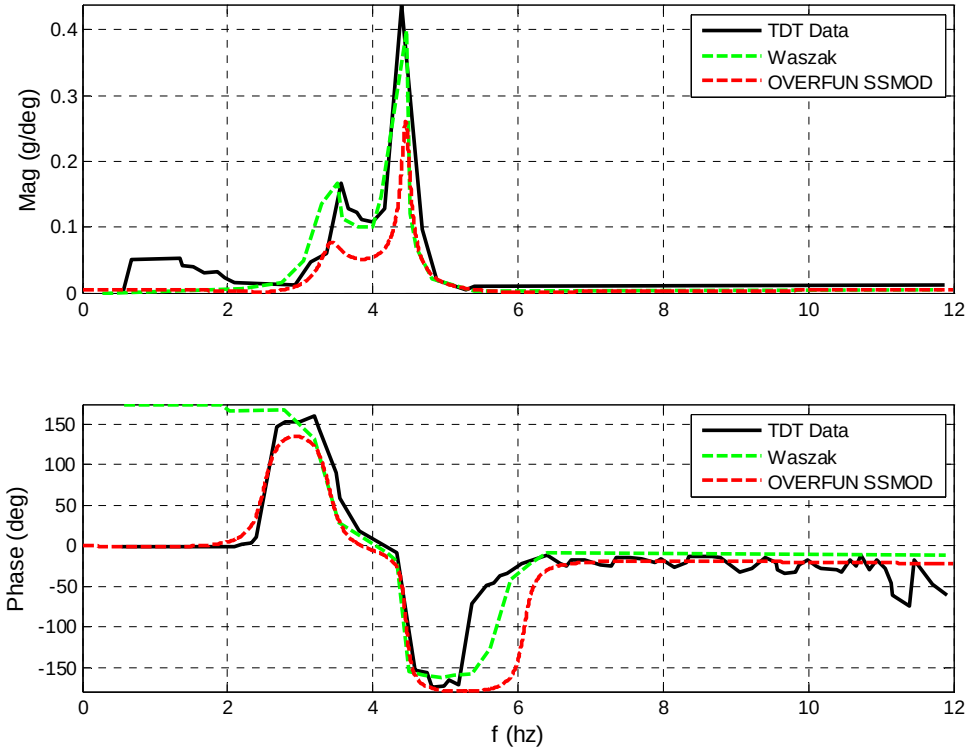

Figure 15: Frequency response of an accelerometer output to the spoiler input of the BACT wing ($q_\infty = 125 psf$; Mach=0.61; AoA=0; Spoiler = 5deg).

6 CONCLUDING REMARKS

In this work we have further extended the wrapper program called OVERFUN to drive the execution of the high fidelity Navier-Stokes solver, FUN3D, leading to the state-space aeroservoelastic model in discrete time.

The newly developed OVERFUN SSMOD module automatically prepares the necessary input files for FUN3D, particularly the structural mode shapes' projections into the wetted surface from the CFD grid, and the namelist input file from a template. The FUN3D generalized aerodynamic force solutions and the modal coordinate excitations or control surface deflections are then collected as system outputs and inputs, respectively, for system identifications. The subspace realization algorithm is utilized to identify the individual aerodynamic systems, i.e., due to the structural deformations (modal coordinates) and the control surface kinematic modes. Thereafter they are integrated with the structural equation of motion represented in modal space and the actuator model to yield the conventional state-space forms of aeroelastic model and plant model.

The Benchmark Active Control Technology (BACT) wing configuration is used as a numerical example to demonstrate the present methodology. The obtained state-space models are used to compute the frequency response of the accelerometer located near the trailing edge of the wing root with respect to the trailing edge flap and the upper spoiler. The results agree favorably well to the wind tunnel test data.

7 ACKNOWLEDGEMENT

The advice of Dr. Walter A. Silva from NASA Langley research center on the work is greatly

appreciated.

8 REFERENCES

[1] ZAERO Theoretical Manual Version 9.0, 2015, ZONA Technology Inc.

[2] Rodden, W.P., Giesing, J.P. and Kalam, T.P., "New Method for Nonplanar Configurations," AGARD Conference Proceeding, CP-80-71, Pt, II, No. 4, 1971.

[3] Yang, S., and Chen, P.C. "Linearized FUN3D for Rapid Aeroelastic Design and Analysis", Presented at International Forum on Aeroelasticity and Structural Dynamics, June 28-July 02, 2015. Saint Petersburg, Russia.

[4] Roger, K. L., "Airplane Math Modeling and Active Aeroelastic Control Design," AGARD-CP-228, 1977, pp. 4.1-4.11.

[5] Karpel, M. "Design for Active and Passive Flutter Suppression and Gust Alleviation," NASA CR-3482, 1981.

[6] Anderson, W. K., and Bonhaus, D. L.: "An Implicit Upwind Algorithm for Computing Turbulent Flows on Unstructured Grids". Compt. and Fluids, Vol. 23, No. 1, pp. 1-21, 1994.

[7] Raveh, D. "CFD-Based Models of Aerodynamic Gust Response". in 47th AIAA/ASME/AHS/ASC Structures, Structural Dynamics, and Materials Conference. 2006. Newport, Rhode Island.AIAA 2006-2022.

[8] Silva, W.A., "Application of Nonlinear Systems Theory to Transonic Unsteady Aerodynamic Responses". Journal of Aircraft, 1993. 30(5): p. 660-668.

[9] Raveh, D.E., "Reduced-Order Models for Nonlinear Unsteady Aerodynamics". AIAA Journal, 2001. 39(8): p. 1417-1429.

[10] Overschee, P.V., and B. De Moor, Subspace Identification for Linear Systems. Dordrecht, Belgium: Kluwer Academic Publisher.

[11] Wang, Z., Sarhaddi, D., and Chen, P.C., "Efficient Clustering Algorithm Using Modal Assurance Criterion for System Identification", 2016 AIAA/ASCE/AHS/ASC Structures, Structural Dynamics, and Materials Conference, AIAA SciTech Forum, (AIAA 2016-1956)

[12] Wang, Z., Yang, S. and Chen, P.C., "Nonlinear Gust Reduced Order Modeling Based On FUN3D And Volterra Theory", 2018 AIAA/ASCE/AHS/ASC Structures, Structural Dynamics, and Materials Conference, AIAA SciTech Forum, (AIAA 2018-1211)

[13] Wang, Z., Yang, S. and Chen, P.C, "Aeroelastic Analysis Using FUN3D-Based ROM Simultaneously Subject to Gust and Control Surface Deflections", AIAA Scitech 2019 Forum, AIAA SciTech Forum, (AIAA 2019-1021)

[14] Bartels, R.E., and Schuster, D.M., "Comparison of Two Navier-Stokes Aeroelastic Methods Using BACT Benchmark Experimental Data," AIAA-99-3157-CP.

[15] Rivera, J.A., Dansberry B.E., Bennett, R.M., Durham, M.H., and Silva, W.A., "NACA 0012 Benchmark Model Experimental Flutter Results with Unsteady Pressure Distributions," AIAA-92-2396-CP.

[16] Waszak, M.R., "Modeling the Benchmark Active Control Technology Wind-Tunnel Model for Application to Flutter Suppression," AIAA-96-3437-CP.

COPYRIGHT STATEMENT